Selective MRI of magnetically labeled cells – a comparative evaluation of positive contrast techniques

J-H. Seppenwoolde[1], R. Oude Engberink[1], A. van der Toorn[1], E. L. Blezer[1], C. J. Bakker[1]

[1]Image Sciences Institute / Dept. of Radiology, University Medical Center Utrecht, Utrecht, Netherlands

Introduction – For the detection and visualization of SPIO-labeled cells or clusters of USPIOs, T2*-weighted imaging is generally used. A clear disadvantage of using T2* weighted techniques is the detection of the cells with negative contrast and signal loss, while signal voids from other sources than cells may be falsely interpreted as signal loss resulting from the presence of labeled cells. A similar problem was found in the passive tracking of endovascular devices, and a solution to this was proposed about 2 years ago [1], as the 'white marker (WM) phenomenon'. In a recent study, the concept of the white marker has been generalized to an extended theoretical and experimental framework, called 'dephased MRI' [2]. The white marker/dephased MRI method can also be applied to detect small clusters of paramagnetic material, as was demonstrated for holmium-loaded microspheres and small paramagnetic elements [3]. The use of this methodology was also realized by Coristine et al [4] who applied the white marker technique for the selective depiction of SPIO labeled cells. Recently, other methods for selective imaging have been proposed and explored, which are primarily alternatives that employ spectrally selective radiofrequency pulses (SSRF) for selective excitation [5] or selective suppression [6] of the longitudinal magnetization. In this work, we describe a basic comparison of three classes of selective MR imaging of field disturbing elements (viz. magnetically labeled entities): the white marker method (WM), the spectrally selective RF method (SSRF) and a newly developed method, the off-resonance balanced gradient-echo method (OBM). Comparison was done by simulations, in vitro experiments, and in vivo rat experiments.

Method – Phantom: as a model of a cluster of labeled cells, a small stainless steel sphere (∅ 0.5 mm, AlSl-316) was mounted in the middle of large bottle, filled with a $MnCl_2$ solution. The bottle was positioned in the iso-center of a clinical 1.5 T MR scanner (Intera NT, Philips Medical Systems). MR imaging: the following general parameters were used. FOV 240x240 mm^2, matrix 256^2, slice thickness 15 mm, 1 signal average, TE 10 ms, volume shimming. Standard gradient echo (GE) and spin-echo (SE) images were made in coronal and transverse direction using TR/flip of 12/15 and 100/90, respectively. *White Marker*: conventional GE was adapted by applying slice dephasing with stepsizes Δk_z from -4 Δk_z to 4 Δk_z. *Spectrally Selective RF*: A standard 2D SE acquisition was adapted by addition of a sinc-shaped saturation pulse before the slice selective excitation (this type of SSRF acts symmetrically around zero, yielding a similar pattern as the WM, whereas the excitation method [5] is one-sided). The bandwidth (BW) of the pulse was varied between 120 and 200 Hz (durations 30 to 50 ms). *Off-resonance balance GE*: after acquisition of a conventional on-resonance excitation scheme with alternating RF pulses ($\beta = \pi$) [7], the frequency of the RF pulses during excitation was shifted. The shift was chosen to set the accumulated phase of the background signal at $\beta = 0$. For maximum shift control, TR was minimized. At a TR of 5 ms, shifts of ± 1, 2, 5 & 10 Hz were given. Simulation: An effective voxel signal was calculated by complex summation of sub-voxel signal contributions (>1000 elements). B_0 and B_1 inhomogeneity were taken into account as well. For WM intra-voxel dephasing is most relevant. For SSRF, the Bloch equations were evaluated for various flip angles and delays. For OBM, non-spoiled, short-TR equations as given in [7] were evaluated. In vivo MR imaging: In 6 rats (Lewis-Hannover), photothrombotic brain lesions were induced and 5 days later, either USPIOs (n=3) or ex vivo-labeled monocytes (n=3) were injected intravenously. The rats were imaged on a 4.7 T machine (Varian, Palo Alto, CA) before and at 1, 3, and 5 days after injection. In addition to standard imaging, the WM and SSRF methods were applied.

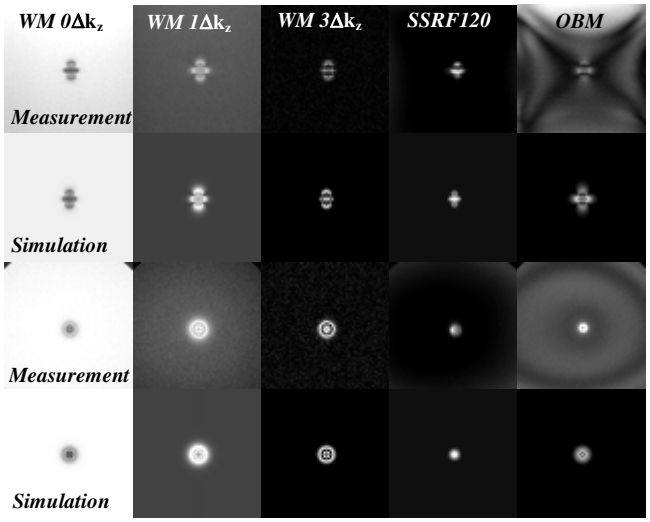

***Figure 1**. Comparison of three selective MRI techniques to visualize a single 'magnetic' element, showing three stages of the WM, the SSRF method, and the OBM for measurement and simulation of images in coronal (upper rows) and transverse direction (lower rows).*

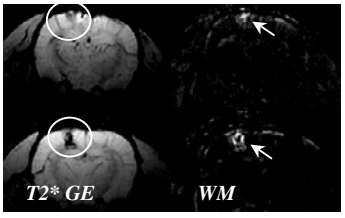

***Figure 2.** Illustration of the WM method applied to two rat brains with laser induced cortical lesions after IV injection of USPIOs (SSRF not shown).*

Results – Fig. 1 illustrates the excellent agreement between simulation and measurement for WM and SSRF and good correspondence for OBM. For the in vivo experiments (Fig 2.), the WM outperformed the SSRF method in visualizing the treated lesions; the lesions were virtually non-visible with the SSRF method, but detectable with WM. Findings of measurements and simulations are summarized in Table 1.

Discussion – The attractiveness of all three selective MRI techniques is that the depiction of magnetically labeled entities like cells with a positive contrast only requires very simple modifications of conventional acquisition schemes and can easily be implemented on any clinical scanner. Each positive contrast technique has its own merits and practical issues (Table 1). Generally spoken, the OBM method has the least flexibility with a very narrow optimum, the SSRF method has more flexibility but may be hampered by RF inhomogeneity and yields relatively small markers, and the WM method has the most flexibility and yields large markers with a very robust contrast. In all methods the background signal can be fully suppressed or partially conserved. During application of WM, one may possibly encounter confusing partial volume effects, which can be corrected for by using symmetrically dephased MRI, a topic beyond the scope of this work.

***Table 1:** Comparison of three classes of positive contrast techniques to selectively visualize para- or ferromagnetic entities like magnetically labeled cells.*

	White Marker / Dephased MRI (WM)	Spectrally selective RF pulse (SSRF)	Off-resonance b-GE (OBM)
Principle	Phase encoding of the MRI signal	Signal preparation with RF pulses	Influencing signal build up
Technique	Dephasing gradients/ gradient imbalances	Spectrally selective saturation RF pulse	Shift of excitation frequency
Type of sequence	Applies to both GE and SE! but GE preferred	Applies to both GE and SE! but SE preferred	GE only, short TR required
Contrast of marker	Sudden transition, followed by robust contrast	Gradual transition with a limited optimum	Very sharp transition, narrow optimum
Marker selectivity	Can be increased by an increase of dephasing	Can be increased by lowering of the BW	Increased by shorter TR & higher flip
Size of 'marker'	Controllable by TE and amount of dephasing, large range of sizes (large size)	Controllable by BW, in practice a limited range of sizes (relatively small size)	Controllable by TR and flip angle (influences balanced GE contrast)
Background signal/contrast	Controlled by amount of dephasing. Can also be non-zero. Dephased MRI contrast (~GE)	Controlled by flip angle of suppression pulse. Can also be chosen non-zero. SE contrast	Due to narrow optimum difficult to control. Balanced GE contrast.
Global field inhomogeneity (B_0)	No influence on marker depiction (WM method is gradient based). Shimming preferred.	Influence on marker depiction (SSRF method is based on B_0 off-set). Shimming required.	Dramatic influence on marker depiction. Shimming crucial.
RF pulse shape or inhomogeneity (B_1)	No significant influence on marker contrast (determined by dephasing)	Influence on marker contrast (by actual 'suppression' of background and 180° pulses)	Influence on marker contrast and size (by variation of effective flip angle)
Speed (no EPI/TSE)	Fast, only limited by TE for certain marker size	Slow, limited by use of 180° pulses and SAR	Very fast, only limited by SAR

Ref: [1] JH Seppenwoolde et al, MRM (2003);50:784 [2] CJG Bakker et al, MRM (accepted) [3] JH Seppenwoolde et al, proc. ISMRM 2003, p1092, [4] AJ Coristine et al, proc ISMRM 2004, p163, [5] CH Cunningham, MRM (2005);53:999 [6] M Stuber, proc ISMRM 2005, p2608. [7] EM Haacke, "Magnetic Resonance Imaging".